Title
Increases in the annual range of soil water storage at northern middle and high latitudes under global warming

Journal
Geophysical Research Letters, 42(10)

ISSN
0094-8276

Authors
Wu, Wen-Ying
Lan, Chia-Wei
Lo, Min-Hui
et al.

Publication Date
2015-05-28

DOI
10.1002/2015gl064110

Peer reviewed

AGU PUBLICATIONS

Geophysical Research Letters

RESEARCH LETTER
10.1002/2015GL064110

Key Points:
- An increase of soil water annual range: Wet (dry) seasons get wetter (drier)
- Stronger heterogeneity in global water distribution under global warming
- Changes in the components in water storage affect soil water seasonality

Supporting Information:
- Figures S1 to S3 and Table S1

Correspondence to:
M.-H. Lo,
minhuilo@ntu.edu.tw

Citation:
Wu, W.-Y., C.-W. Lan, M.-H. Lo, J. T. Reager, and J. S. Famiglietti (2015), Increases in the annual range of soil water storage at northern middle and high latitudes under global warming, *Geophys. Res. Lett.*, *42*, 3903–3910, doi:10.1002/2015GL064110.

Received 3 APR 2015
Accepted 7 MAY 2015
Accepted article online 11 MAY 2015
Published online 29 MAY 2015

Increases in the annual range of soil water storage at northern middle and high latitudes under global warming

Wen-Ying Wu[1], Chia-Wei Lan[1], Min-Hui Lo[1], John T. Reager[2], and James S. Famiglietti[2,3]

[1]Department of Atmospheric Sciences, National Taiwan University, Taipei, Taiwan, [2]NASA Jet Propulsion Laboratory, California Institute of Technology, Pasadena, California, USA, [3]Department of Earth System Science and Department of Civil and Environmental Engineering, University of California, Irvine, California, USA

Abstract Soil water storage is a fundamental signal in the land hydrological cycle and changes in soil moisture can affect regional climate. In this study, we used simulations from Coupled Model Intercomparison Project Phase 5 archives to investigate changes in the annual range of soil water storage under global warming at northern middle and high latitudes. Results show that future warming could lead to significant declines in snowfall, and a corresponding lack of snowmelt water recharge to the soil, which makes soil water less available during spring and summer. Conversely, more precipitation as rainfall results in higher recharge to soil water during its accumulating season. Thus, the wettest month of soil water gets wetter, and the driest month gets drier, resulting in an increase of the annual range and suggesting that stronger heterogeneity in global water distribution (changing extremes) could occur under global warming; this has implications for water management and water security under a changing climate.

1. Introduction and Background

The water stored in soils beneath the land surface is important in numerous physical processes, including supporting runoff generation, land-atmosphere exchanges, and modulating flood potential [*Reager et al.*, 2014] and drought duration [*Thomas et al.*, 2014]. Climate-driven changes in the hydrological cycle can lead to changes in extremes of precipitation, soil moisture, and surface water [*Taylor et al.*, 2013], which can affect food and water security as well as plant growth. *Chou and Lan* [2012] and *Chou et al.* [2013] indicated that the seasonal range of precipitation tends to increase under global warming, specifically, that wet seasons become wetter, and that dry seasons get drier. Studies have shown the effects of climate change on terrestrial hydroclimatology as well. For example, *Gregory et al.* [1997] used the HadCM2 climate model to show that a rise in greenhouse gas concentrations was related to decreases in soil moisture in the Northern Hemisphere middle latitudes because of the reduced snow cover causing higher evaporation during the winter and spring. Furthermore, warmer temperatures are able to alter the phase of precipitation (i.e., less winter precipitation falls as snow) and to cause earlier runoff peak in the spring [*Barnett et al.*, 2005]. *Dirmeyer et al.* [2013] reported an increase in the interannual variability of soil water storage over most of the high latitudes in the Representative Concentration Pathway (RCP) 8.5 projections from the Coupled Model Intercomparison Project Phase 5 (CMIP5) archives [*Taylor et al.*, 2012]. They also suggested that terrestrial hydrological-state variables (such as soil moisture) have a more dominant role, compared with that of the free atmosphere, in boundary layer properties under climate changes.

Recently, *Kumar et al.* [2014] found more water availability in the wet season and less water availability in dry season for most parts of the world under a changing climate. Analyzing CMIP5 outputs, *Arnell and Lloyd-Hughes* [2014] showed that the impacts of global warming on water resource stress and river flooding under RCP 8.5 were greater than those of other RCPs in the future climate. In addition, *Zhang et al.* [2014] indicated that both the wetter area (where the runoff increase exceeds 10%) and the drier area (where the runoff decrease exceeds 10%) approximately linearly increased with the rise in the global mean temperature, indicating more spatially heterogeneous soil wetness over the land.

Under climate change, the availability of river runoff may decrease in existing water-stressed regions [*Milly et al.*, 2005]. Changes in soil water storage also affect the amount of groundwater-driven runoff [e.g., *Lo et al.*, 2008], which is a vital water resource under climate changes. How land water storage responds to

climate change is still relatively unknown and is of value to explore, especially the seasonal variations of soil water storage, since larger seasonal variations coupled with the highly nonlinear relationship between atmospheric-hydrological fluxes and storages [e.g., *Famiglietti and Wood*, 1994; *Kollet and Maxwell*, 2008] could lead to unexpected consequences such as more extreme events. The lack of global observations on land water storage makes it difficult to examine how terrestrial water storage changes globally under the changing climate.

Observations of total water storage (TWS) have only recently become available. Beginning in 2002, the Gravity Recovery and Climate Experiment (GRACE) mission [*Tapley et al*., 2004] is able to provide highly accurate maps of changes in TWS for monthly and longer timescales both over the land [*Swenson et al*., 2003] and ocean [*Chambers et al*., 2004]. The GRACE mission now provides estimates of variations in terrestrial water storage for areas larger than approximately 150,000 km^2 (approximately $4° \times 4°$ near the equator) [*Swenson et al*., 2006]. Several previous studies have compared GRACE observations of terrestrial water storage to in situ observations [*Rodell et al*., 2004; *Swenson et al*., 2006] and models [*Ramillien et al*., 2004; *Syed et al*., 2008], with reasonable agreement. The CMIP5 archives have been utilized to explore how land water availability responds to climate change [e.g., *Kumar et al*., 2014]. In this study, we used GRACE data to select CMIP5 models, in which simulation outputs are used for the examination of changes in global land-soil-water storage (the sum of soil water in all layers) from 2011 to 2100. In addition to the mean climatology of the terrestrial water cycle, the shifts and changes in the magnitude of the seasonal cycle are essential to water management. Hence, we focused more on the amplitude of the seasonal cycle, which we simply call the "annual range" and represents the dominant time scale for the variability of water storage [*Güntner et al*., 2007]. We name the period when storage falls the "declining season," and the period when storage increases, the "accumulating season."

2. Data and Model

We use monthly hydrological outputs in the RCP 8.5 future-warming scenario from the CMIP5 archives, corresponding to a radiation forcing of 8.5 W/m^2 in the year of 2100 (relative to that of the preindustrial period). The CMIP5 project involves an abundance of Earth system model experiments worldwide. Based on the available outputs in the CMIP5 archives, we defined TWS over land as the sum of the amount of snow and soil water storage. The "true" TWS in nature includes groundwater, surface water, and glaciers, which are not fully included in current Earth system models. However, groundwater tends to contribute more to the interannual variability of TWS variations than to the seasonal variability [*Güntner et al*., 2007]. The National Center for Atmospheric Research Community Land Model version 4 [*Lawrence et al*., 2011] sensitivity tests also indicated that the seasonality of global, averaged groundwater variations was relatively low compared with that of soil water and snow water equivalent (results not shown). In addition, CMIP5 standard outputs include only snow water equivalent and soil water storage. Consequently, we use snow water equivalent (SNW) and soil water storage (MRSO, which are used in the CMIP5 archives and included water in all phases for all the soil layers) to represent the TWS.

Recent releases (RL05) of GRACE data [*Landerer and Swenson*, 2012] from the Center for Space Research at the University of Texas at Austin are used for the comparisons with the CMIP5 model output. The global average of land water storage excludes Antarctica and Greenland. In addition, for Figures 2–5, grid cells near the coast with land fractions under 99% were removed. The annual range is defined as the difference between the maximal and the minimal TWS for each year. We use δTWS to represent the annual range of total water storage, δSNW to represent the annual range of snow water equivalent, and δMRSO to represent the annual range of soil water storage in this study.

3. Results

3.1. Selection of CMIP5 Models

The configurations of soil layer representations in each land surface model from the CMIP5 archives are extremely diverse, depending on the complexity of the model, soil depth, and whether a saturated component is included. Thus, some models have a simulated TWS that is unrealistic, in which the seasonal cycle may even be out of phase. A Taylor diagram provides a statistical summary of how well patterns match each other and is typically used to compare the simulated data with observations [*Taylor*, 2001].

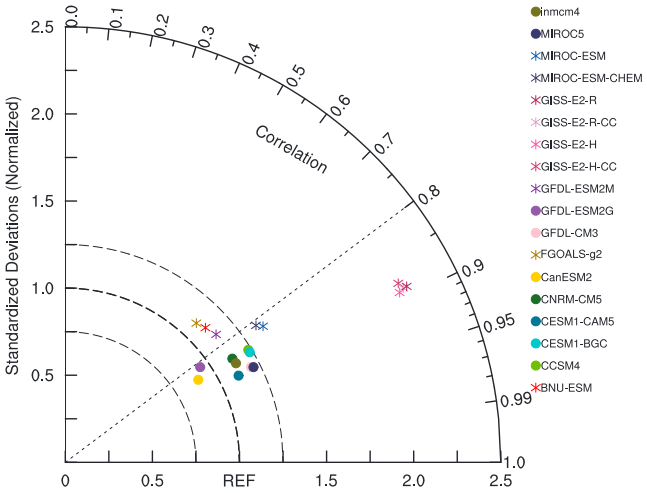

Figure 1. Normalized Taylor diagram presents a comparison of the GRACE observations with the CMIP5 simulations for the monthly time series of global land water storage for 2006 to 2010. The diagram shows the correlation and ratio of the standard deviation. The filled circles represent the models that were relatively similar to the observations, had complete outputs in the CMIP5 archives, and were used in this analysis.

Figure 1 shows a comparison of the globally averaged monthly time series (2006–2010) from models and from the GRACE observations. The correlation coefficients for the radial line denote the relationship between GRACE and the model simulations, indicating similarities on seasonal and interannual time scales. Standard deviations on the *x* and *y* axes quantify the variance between the two time series; the normalized standard deviation (the standard deviation of the time series of the model divided by that of the GRACE observations) is higher than 1, indicating that the variability of the data in the model simulations is higher than that in the GRACE observations. The points inside the bold, curved line mean that the model simulations have lower variability than the GRACE observations. To select the CMIP5 models used in this study, we first excluded the models without completed output records for precipitation, evaporation, runoff, snow water equivalent, snowfall, snowmelt, and soil frozen water. Then, we established two criteria from the Taylor diagram in Figure 1: (1) a correlation coefficient ≥ 0.8 (p value < 0.01) and (2) a normalized standard deviation $\leq 1 \pm 0.25$ to further remove the models based on GRACE TWS, thereby reducing the number of models from 18 to 9 (the models with the filled circles in Figure 1). The details of the selected nine models are listed in Table S1 in the supporting information, and the spatial distribution of the standard deviation for the 18 models and GRACE is shown in Figures S1–S3.

3.2. Changes in Annual Range of Land Water Storage Under Global Warming

Figure 2a shows the time series of globally averaged δTWS from the ensemble mean of the nine models; the annual range is defined as the difference between the maximal (approximately April) and the minimal (approximately September) TWS for each year. The gray shading denotes the single standard deviation range, and the anomaly indicates removing the mean of the first 10 years (2011–2020). Figure 2a shows that the annual range of global TWS has no significant trend under global warming, and Figure 2c also indicates that the trends for the TWS annual range are rather diverse among the nine models. However, once partitioned, the soil water storage and snow water equivalent have significant trends ($p < 0.05$) in the annual range from 2011 to 2100 (Figure 2b). Every model has a consistently declining trend for annual range of snow water equivalent and a consistently increasing trend for annual range of soil water (Figure 2c). Note that the seasonal cycles of global snow and soil water storage are similar to that of the TWS with a sine-shaped wave within a year; therefore, when we defined the annual range of soil water and snow water equivalent in Figures 2b and 2c, we used the months of maximal and minimal TWS to be consistent with Figure 2a for analyzing the contributions to δTWS.

Figure 3a shows the changes in seasonal cycle anomalies for soil water storage. The blue line represents the multimodel mean of seasonal cycle anomalies from 2011 to 2020; the red line represents 2091 to 2100. The anomalies were computed by removing from the means of 2011 to 2020 and 2091 to 2100, respectively. Figure 3a shows that the peak of soil water storage is in April and that the lowest is in September; the error bar shows a single standard deviation among models. Figure 3a clearly shows a larger seasonal cycle at the end of this century, which is consistent with that observed in Figure 2b. Figures 3b–3e show changes in the seasonal cycle for different latitudinal zones. In 30°S to 0° and 0° to 30°N, the standard deviation among models slightly increases under global warming, but there is no significant change in the annual cycle. However, in 30°N to 60°N (Figure 3d), the change in the seasonal cycle is extremely clear and indicates that this region contributes substantially to the change in the

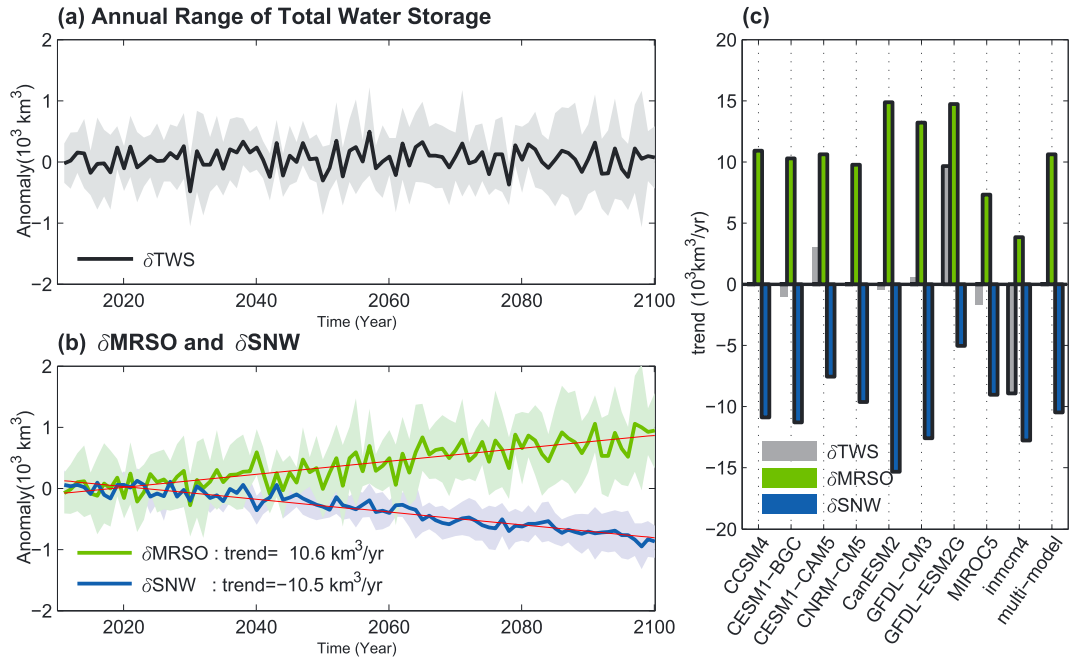

Figure 2. (a) Time series of the annual range for the global, averaged TWS from the ensemble mean of the nine models. The annual range is defined as the difference between the maximal and the minimal TWS for each year. (b) The same as Figure 2a but for soil water storage (δMRSO) and snow water equivalent (δSNW). Shaded areas represent a single standard deviation among models. (c) A linear TWS trend (gray) corresponds to the soil water storage (green) and snow amount (blue) for 2011 to 2100 (RCP 8.5). The trend with a 95% confidence interval is marked with an edge.

seasonal cycle of global soil water storage. The annual range also exhibits a slight increase over the zonal mean of 60°N to 90°N, as shown in Figure 3e.

Figure 3f shows the global patterns, including the number of models exhibiting annual range increases (a positive value) or decreases (a negative value) of soil water storage, between the two decades from 2011 to 2020 and from 2091 to 2100. For example, the grid with a number "9" in Figure 3f indicates that all of the models exhibited increases in the annual range of soil water storage. As shown in Figure 3f, the major regions having an increasing seasonal cycle of soil water storage exist over the middle and high latitudes of the Northern Hemisphere. The resulting pattern agrees with Figures 3a–3e. To further diagnose contributions of snow water equivalent to the soil water storage, we defined the snow cover regions with the criterion of 0.5 mm snow water equivalent in the first decade and the edge is presented in the red line in Figure 3f. It shows overall increases in annual range of soil water storage exist over snow cover regions, revealing the importance of snow effects on the soil water storage. However, over the regions without snow cover, no comprehensive changes are observed, which is also consistent with the strongly heterogeneous distributions of the annual range of soil water as shown in Figure 3f.

Under global warming, deceases in snowfall results in less snow water equivalent in most regions globally (Figure 4a), except some extreme cold regions such as Northeastern Siberia where snowfall, in fact, increases [*Adam et al.*, 2009]. Changes in the annual range of snow water equivalent (Figure 4b) have similar patterns to the mean changes (Figure 4a), because lack of snowfall in winter causes less snow water equivalent and less snowmelt consequently in the spring and summer. In addition, warming leads to overall less soil frozen water (Figure 4c) with decreases in its annual range in most regions (Figure 4d), despite Northeastern Siberia and Arctic of Canada, where the annual range of soil frozen water still increases. That is because of the deepening active layer located above the continuous permafrost with larger temperature amplitude which impacts the seasonal processes of thawing in the summer and freezing again in the autumn/winter under global warming [*Koven et al.*, 2013]. This also implies that changes in the soil hydrology are crucial to increases in the annual range of soil water storage over Northeastern Siberia and Arctic of Canada.

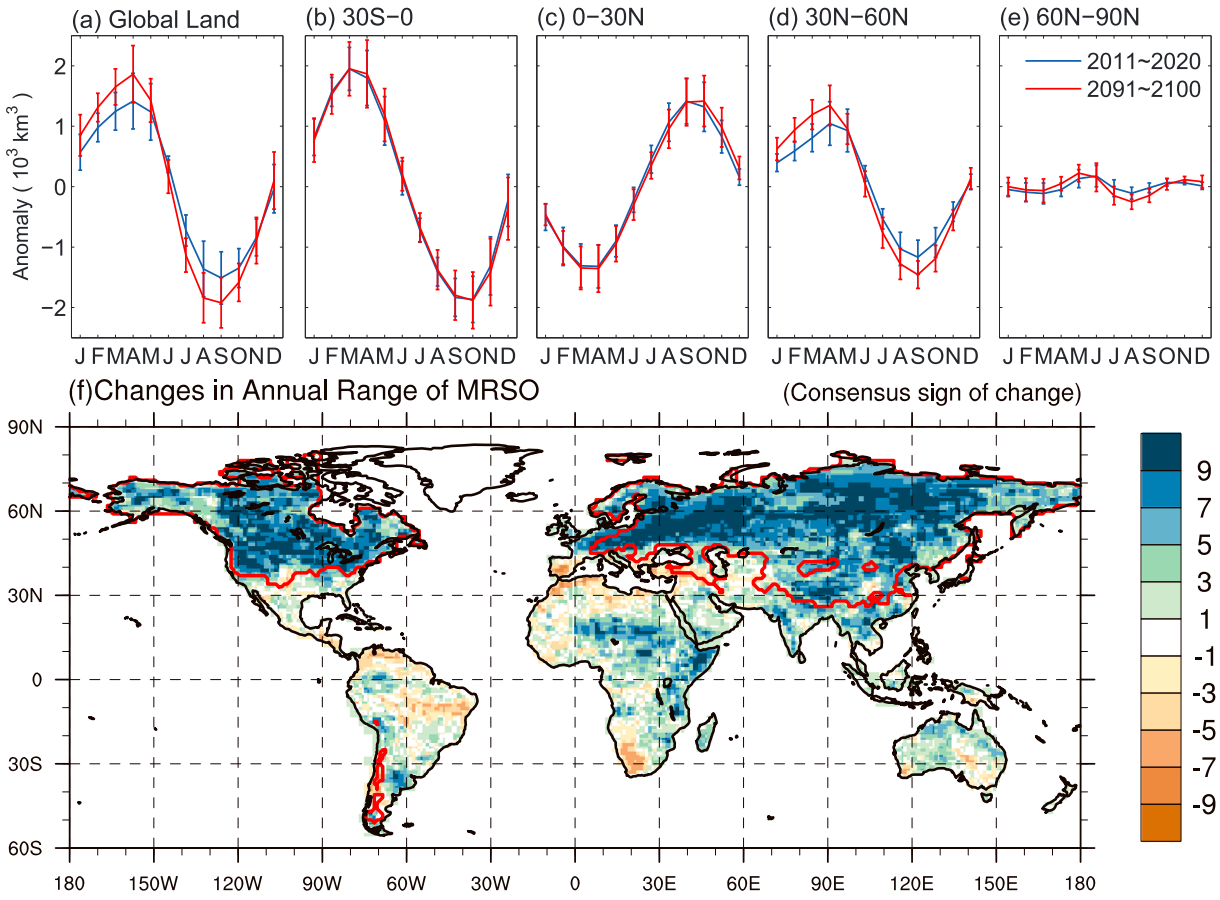

Figure 3. (a) Global mean of the changes in the seasonal cycle anomalies of soil water storage. Figures 3b–3e show the changes in seasonal cycle at different latitude zones from (b) 30°S to 0°, (c) 0° to 30°N, (d) 30°N to 60°N, and (e) 60°N to 90°N. A blue/red line shows the seasonal cycle anomalies of first/last decade (2011–2020/2091–2100) relative to the mean in each period. The error bar shows a single standard deviation among models. (f) The sign and degree of consensus among the nine climate models for changes in δMRSO from 2011 to 2020 and 2091 to 2100. Red line shows the multimodel snow cover region.

Over northern middle and high latitudes, decreases in snowfall (Figure 5b) result in a lower level of snow water equivalent (Figure 5d). Less snowmelt (Figure 5c) in the declining season leads to a deficient supply of soil water storage, resulting in a dry season that is drier (i.e., a larger seasonal cycle). Whereas snowmelt and the frozen soil in the shallow soil layer are decreasing, more precipitation is in the form of liquid water (Figure 5a); consequently, access to water directly supplied by rainfall increases soil water storage in the accumulating season at high latitudes in Northern Hemisphere. In summary, changes in the partitioning of precipitation into snowfall and rainfall result in higher recharge in the accumulating season but lower recharge in the declining season of snowmelt, resulting in a larger seasonal cycle. More rainfall results in higher recharge to soil water. Moreover, since the soil frozen water is able to prevent infiltration [*Niu and Yang*, 2006], melting of soil frozen water induces more potential capacity of soil water storage and allows more liquid water to infiltrate so that the seasonal cycle of soil water storage increases as well.

Additionally, Figure 5f shows the scatterplot of the changes between the periods of 2091 to 2100 and 2011 to 2020 for the mean surface temperature over land and annual range of soil water storage over 30°N to 90°N for each model. The models with larger changes in surface temperature have more increases in the annual range of soil water storage with a correlation coefficient of 0.83. A linear fit in Figure 5f indicates an increase rate of 326 km^3/°C, which is approximately 14% of the annual range of MRSO over northern middle and high latitudes. Hence, annual range of MRSO not only increases with the temperature in each model but also has a positive response to increases in the temperature across models. The larger annual range of soil water storage might lead to an increased risk of flood and drought and has implications for

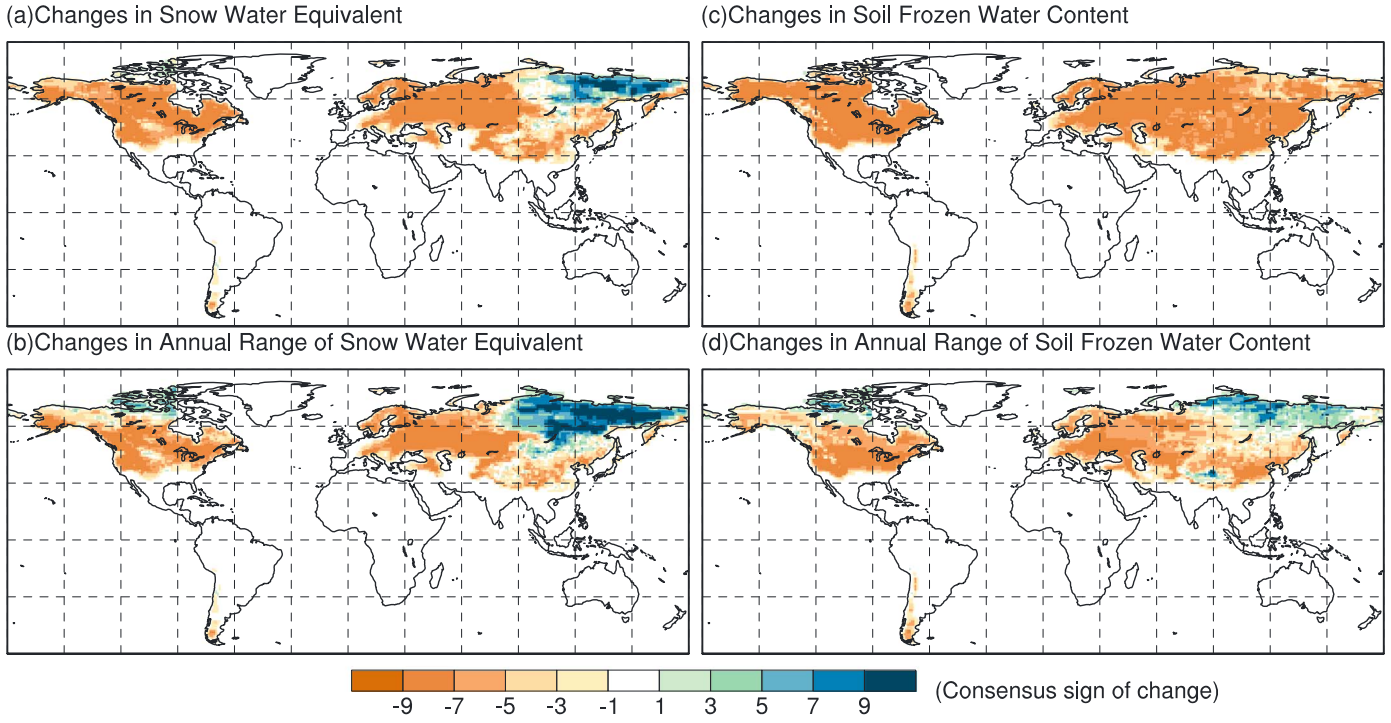

Figure 4. The same as Figure 3f but for (a) mean snow water equivalent, (b) annual range of snow water equivalent, (c) mean soil frozen water content, and (d) annual range of soil frozen water content.

changing extremes. Some of the models from the CMIP5 archives showed a maximum shift of soil water storage to approximately 1 month earlier after warming. However, most of the climate models have not considered glaciers, ice sheets, and the correct permafrost characteristics, which also limit the findings in this study.

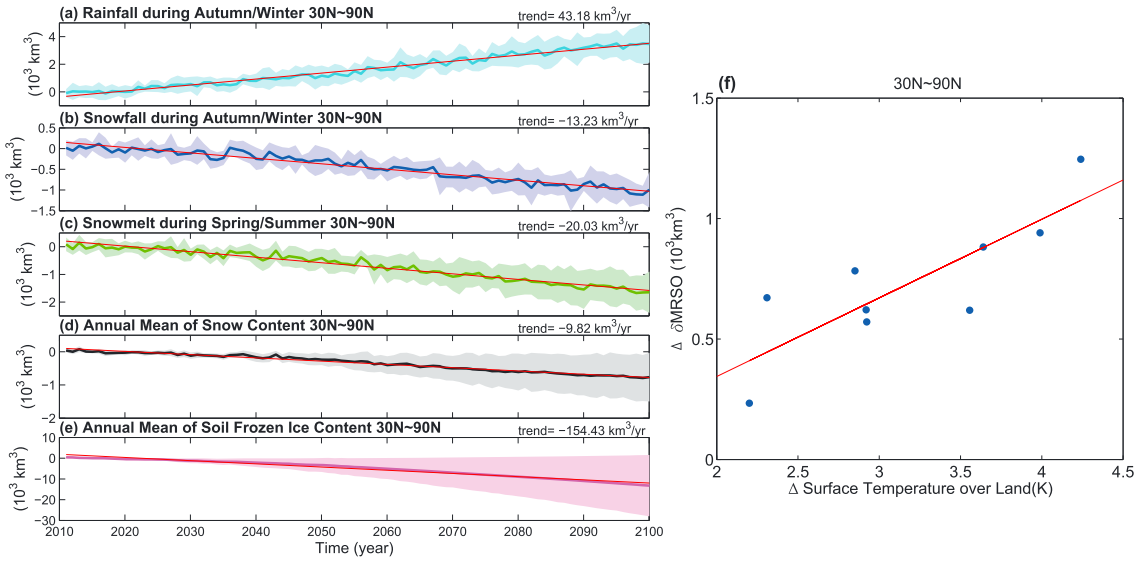

Figure 5. The multimodel mean of (a) rainfall in September–February (SONDJF), (b) snowfall in SONDJF, (c) snowmelt in March–August (MAMJJA), (d) annual snow water equivalent amounts, and (e) annual soil ice amounts over 30°N to 90°N relative to the mean of 2011 to 2020. The shaded areas represent a single standard deviation among models. (f) Relationship between the annual mean of surface temperature over land and annual range of soil water storage from changes between the periods of 2091 to 2100 and 2011 to 2020 of each model over 30°N to 90°N.

4. Conclusions

Results from the CMIP5 analyses showed potential impacts of global warming on terrestrial water storage. Despite a water cycle that is intensifying through faster water transport and stronger heterogeneous distribution of precipitation under global warming [e.g., *Chou et al.*, 2009], the interaction of changes in the components in terrestrial water storage, such as partitioning into snow water equivalent or soil moisture and partitioning into liquid water or ice in the soil, may also play a crucial role. An increasing temperature at high latitudes and elevations, where snow and land ice exist, leads to a loss of snow on the surface and soil frozen water in the cryosphere. Increases in temperature and declines in snowpack and snowmelt during the spring and summer result in lower recharge to soil water storage, which makes soil water storage less available over most of the middle and high latitudes of the Northern Hemisphere. Lower levels of water during the dry season have more formidable consequences for agricultural activities because of increases in the demand for irrigation water [*Wada et al.*, 2013]. In addition, under warming, the ratio of liquid water flux to total precipitation becomes higher; thus, more rainfall results in higher recharge to soil water storage during the accumulating season. Thus, the wettest month (approximately April) gets wetter, and the driest month (approximately September) gets drier, resulting in an increase of the annual range under global warming. The increase in the annual range of soil water under global warming could affect future water resource management, plant adaption, and agriculture, especially over the snow-dominant regions where more than 1 billion people live [*Barnett et al.*, 2005].

Acknowledgments

We acknowledge the World Climate Research Programme's Working Group on Coupled Modelling, which is responsible for CMIP, and we thank the climate modeling groups for producing and making available their model output. For CMIP, the U.S. Department of Energy's Program for Climate Model Diagnosis and Intercomparison provides coordinating support and led development of software infrastructure in partnership with the Global Organization for Earth System Science Portals. GRACE land data were processed by Sean Swenson, supported by the NASA MEaSUREs Program, and are available at http://grace.jpl.nasa.gov. This study was supported by the MOST 103-2111-M-002-006 and MOST 104-2923-M-002-002-MY4 to National Taiwan University. A portion of this research was conducted at the Jet Propulsion Laboratory, California Institute of Technology, under a contract with NASA.

The Editor thanks Sanjiv Kumar and an anonymous reviewer for their assistance in evaluating this paper.

References

Adam, J. C., A. F. Hamlet, and D. P. Lettenmaier (2009), Implications of global climate change for snowmelt hydrology in the twenty-first century, *Hydrol. Processes*, *23*(7), 962–972.

Arnell, N. W., and B. Lloyd-Hughes (2014), The global-scale impacts of climate change on water resources and flooding under new climate and socio-economic scenarios, *Clim. Change*, *122*(1–2), 127–140.

Barnett, T. P., J. C. Adam, and D. P. Lettenmaier (2005), Potential impacts of a warming climate on water availability in snow-dominated regions, *Nature*, *438*(7066), 303–309.

Chambers, D. P., J. Wahr, and R. S. Nerem (2004), Preliminary observations of global ocean mass variations with GRACE, *Geophys. Res. Lett.*, *31*, L13310, doi:10.1029/2004GL020461.

Chou, C., and C.-W. Lan (2012), Changes in the annual range of precipitation under global warming, *J. Clim.*, *25*(1), 222–235, doi:10.1175/JCLI-D-11-00097.1.

Chou, C., J. D. Neelin, C.-A. Chen, and J.-Y. Tu (2009), Evaluating the "rich-get-richer" mechanism in tropical precipitation change under global warming, *J. Clim.*, *22*, 1982–2005, doi:10.1175/2008JCLI2471.1.

Chou, C., J. C. H. Chiang, C.-W. Lan, C.-H. Chung, Y.-C. Liao, and C.-J. Lee (2013), Increase in the range between wet and dry season precipitation, *Nat. Geosci.*, *6*(4), 263–267.

Dirmeyer, P. A., Y. Jin, B. Singh, and X. Yan (2013), Trends in land–atmosphere interactions from CMIP5 simulations, *J. Hydrometeorol.*, *14*(3), 829–849.

Famiglietti, J., and E. Wood (1994), Multiscale modeling of spatially variable water and energy balance processes, *Water Resour. Res.*, *30*(11), 3061–3078, doi:10.1029/94WR01498.

Gregory, J. M., J. F. B. Mitchell, and A. J. Brady (1997), Summer drought in northern midlatitudes in a time-dependent CO_2 climate experiment, *J. Clim.*, *10*(4), 662–686.

Güntner, A., J. Stuck, S. Werth, P. Döll, K. Verzano, and B. Merz (2007), A global analysis of temporal and spatial variations in continental water storage, *Water Resour. Res.*, *43*, W05416, doi:10.1029/2006WR005247.

Kollet, S. J., and R. M. Maxwell (2008), Capturing the influence of groundwater dynamics on land surface processes using an integrated, distributed watershed model, *Water Resour. Res.*, *44*, W02402, doi:10.1029/2007WR006004.

Koven, C. D., W. J. Riley, and A. Stern (2013), Analysis of permafrost thermal dynamics and response to climate change in the CMIP5 Earth System models, *J. Clim.*, *26*(6), 1877–1900, doi:10.1175/JCLI-D-12-00228.1.

Kumar, S., D. M. Lawrence, P. A. Dirmeyer, and J. Sheffield (2014), Less reliable water availability in the 21st century climate projections, *Earth's Future*, *2*(3), 152–160.

Landerer, F. W., and S. C. Swenson (2012), Accuracy of scaled GRACE terrestrial water storage estimates, *Water Resour. Res.*, *48*, W04531, doi:10.1029/2011WR011453.

Lawrence, D. M., et al. (2011), Parameterization improvements and functional and structural advances in version 4 of the Community Land Model, *J. Adv. Model. Earth Syst.*, *3*(1), M03001, doi:10.1029/2011MS00045.

Lo, M.-H., P. J. F. Yeh, and J. S. Famiglietti (2008), Constraining water table depth simulations in a land surface model using estimated baseflow, *Adv. Water Resour.*, *31*(12), 1552–1564.

Milly, P. C. D., K. A. Dunne, and A. V. Vecchia (2005), Global pattern of trends in streamflow and water availability in a changing climate, *Nature*, *438*(7066), 347–350.

Niu, G.-Y., and Z.-L. Yang (2006), Effects of frozen soil on snowmelt runoff and soil water storage at a continental scale, *J. Hydrometeorol.*, *7*(5), 937–952.

Ramillien, G., A. Cazenave, and O. Brunau (2004), Global time variations of hydrological signals from GRACE satellite gravimetry, *Geophys. J. Int.*, *158*(3), 813–826.

Reager, J. T., B. F. Thomas, and J. S. Famiglietti (2014), River basin flood potential inferred using GRACE gravity observations at several months lead time, *Nat. Geosci.*, *7*(8), 588–592.

Rodell, M., J. S. Famiglietti, J. Chen, S. I. Seneviratne, P. Viterbo, S. Holl, and C. R. Wilson (2004), Basin scale estimates of evapotranspiration using GRACE and other observations, *Geophys. Res. Lett.*, *31*, L20504, doi:10.1029/2004GL020873.

Swenson, S., J. Wahr, and P. C. D. Milly (2003), Estimated accuracies of regional water storage variations inferred from the Gravity Recovery and Climate Experiment (GRACE), *Water Resour. Res.*, *39*(8), 1223, doi:10.1029/2002WR001808.

Swenson, S., P. J. F. Yeh, J. Wahr, and J. Famiglietti (2006), A comparison of terrestrial water storage variations from GRACE with in situ measurements from Illinois, *Geophys. Res. Lett.*, *33*, L16401, doi:10.1029/2006GL026962.

Syed, T. H., J. S. Famiglietti, M. Rodell, J. Chen, and C. R. Wilson (2008), Analysis of terrestrial water storage changes from GRACE and GLDAS, *Water Resour. Res.*, *44*, W02433, doi:10.1029/2006WR005779.

Tapley, B. D., S. Bettadpur, M. Watkins, and C. Reigber (2004), The gravity recovery and climate experiment: Mission overview and early results, *Geophys. Res. Lett.*, *31*, L09607, doi:10.1029/2004GL019920.

Taylor, K. E. (2001), Summarizing multiple aspects of model performance in a single diagram, *J. Geophys. Res.*, *106*(D7), 7183–7192, doi:10.1029/2000JD900719.

Taylor, K. E., R. J. Stouffer, and G. A. Meehl (2012), An overview of CMIP5 and the experiment design, *Bull. Am. Meteorol. Soc.*, *93*(4), 485–498, doi:10.1175/BAMS-D-11-00094.1.

Taylor, R. G., et al. (2013), Ground water and climate change, *Nat. Clim. Change*, *3*(4), 322–329.

Thomas, A. C., J. T. Reager, J. S. Famiglietti, and M. Rodell (2014), A GRACE-based water storage deficit approach for hydrological drought characterization, *Geophys. Res. Lett.*, *41*, 1537–1545, doi:10.1002/2014GL059323.

Wada, Y., et al. (2013), Multimodel projections and uncertainties of irrigation water demand under climate change, *Geophys. Res. Lett.*, *40*, 4626–4632, doi:10.1002/grl.50686.

Zhang, X., Q. Tang, X. Zhang, and D. P. Lettenmaier (2014), Runoff sensitivity to global mean temperature change in the CMIP5 Models, *Geophys. Res. Lett.*, *41*, 5492–5498, doi:10.1002/2014GL060382.